Superinfection exclusion: a viral strategy with short-term benefits and long-term drawbacks

Michael Hunter[1,*] **and Diana Fusco**[1,**]

[1]Cavendish Laboratory, University of Cambridge, Cambridge, CB3 0HE, United Kingdom
[*]mth47@cam.ac.uk
[**]df390@cam.ac.uk

ABSTRACT

Viral superinfection (co-infection) occurs when multiple viral particles infect the same host. In nature, several viral species are found to have evolved diverse mechanisms to prevent superinfection (superinfection exclusion) but how this strategic choice impacts the fate of mutations in the viral population remains unclear. Using stochastic simulations, we find that genetic drift is suppressed when superinfection occurs, thus facilitating the fixation of beneficial mutations and the removal of deleterious ones. Interestingly, we also find that the competitive (dis)advantage associated with variations in life history parameters is not necessarily captured by the viral growth rate for either infection strategy. Putting these together, we then show that a mutant with superinfection exclusion will easily overtake a superinfecting population even if the latter has a much higher growth rate. Our findings suggest that while superinfection exclusion can negatively impact the long-term adaptation of a viral population, in the short-term it is ultimately a winning strategy.

Introduction

Bacteriophages (phages) are viruses that infect and replicate within bacteria. Much like many other viruses, reproduction in lytic phage is typically characterised by several key steps: adsorption to a host cell, injection of the viral genetic material, hijacking of the host machinery, intracellular production of new phage, and finally, the release of progeny upon cell lysis. Phages represent one of the most ubiquitous and diverse organisms on the planet, and competition for viable host can lead to different strains or even species of phage superinfecting (or co-infecting) the same bacterial cell, ultimately resulting in the production of more than one type of phage (Fig. 1a)[1,2]. Interestingly, several phages have evolved mechanisms that prevent superinfection (superinfection exclusion). This can be achieved at the early stage of infection, by preventing further adsorption of phage, or at a later stage, by preventing the successful injection of subsequent phage DNA[3,4]. For instance, bacteriophage T5 encodes a lipoprotein (Llp) that is synthesised by the host at the start of infection and prevents further adsorption events by blocking the outer membrane receptor site (FhuA protein)[5,6]. Bacteriophage T4 encodes two proteins, Imm and Sp, that prevent superinfection by other T-even phages by inhibiting the degradation of bacterial peptidoglycan, whose presence hinders the DNA transfer across the membrane[7,8].

Given that populations which allow and prevent superinfection both exist in the wild, it is natural to wonder what impact either strategy has on the evolution of viral populations. This question has been studied in various systems from the perspective of intracellular interactions and competition[9–16]. Superinfection allows for the exchange of genetic material between viruses through recombination, which can increase diversity and improve the efficiency of selection, but may also decrease fitness by promoting the presence of deleterious mutants at low frequencies[17–19]. Additionally, in RNA viruses with segmented genomes, superinfection can lead to hybrid offspring containing re-assorted mixtures of the parental segments (reassortment). This mechanism can in principle improve selection efficiency, as re-assorted segments may generate highly deleterious variants that will be easily outcompeted by the rest of the population[20]. Superinfection can also lead to viral complementation, where defective viruses can benefit from superior products generated by ordinary viruses inside the host[20–24]. This process increases the diversity of the population, but also allows cheating individuals to persist in the viral population for long times[20,21].

A necessary condition for superinfection is a multiplicity of infection (MOI) greater than one, and several experimental systems have been used to study the impact of MOI on viral dynamics[22,23,25–29]. For instance, high MOI in RNA phage $\phi 6$ has been shown to result in a behaviour conforming to the Prisoner's Dilemma strategy in game theory, and a reduction in viral diversity[25–28,30]. Theoretically, this question has been investigated in different scenarios[31], in particular in the context of human immunodeficiency virus (HIV) infections[17,18,32–37]. These studies have focused on determining whether superinfection preferentially occurs simultaneously or sequentially, in an effort to explain experimental data, and on the role of recombination in the acquisition of drug resistance, showing that its impact depends on the effective population size. The role of MOI has also

been studied in terms of diversity and evolution of the viral population[17,18,34,38–43], with theoretical predictions suggesting that superinfection favours increased virulence, and that within-host interactions can lead to a more diverse population.

Despite the active work in the area, several fundamental questions on the role of superinfection exclusion on viral dynamics remain unanswered. First, while decreasing MOI in viral populations that allow superinfection decreases the *likelihood* of superinfection, it does not introduce a superinfection exclusion mechanism that prevents superinfection altogether, making it difficult to draw conclusions about the dis(advantages) of this viral strategy. Second, little is known about how the simple occurrence of superinfection, before even accounting for the additional effects of any intracellular interactions, impacts the evolution of viral populations, particularly when it comes to fundamental evolutionary outcomes such as mutant fixation probabilities. A quantitative understanding of this baseline behaviour is necessary to evaluate the impact of the many additional intracellular interactions that can occur (recombination, defective viruses, etc.). The limited work in this area has shown that in the absence of intracellular interactions, high MOI in superinfecting viral populations can promote the presence of disadvantageous mutants in the "short term," and obstruct it in the "long term"[44,45], but how the evolutionary outcomes in each case depend on the parameters describing the viral life-cycle (adsorption rate, lysis time and burst size) and the dis(advantages) of either strategy remain unclear.

Here, we investigate how allowing or preventing superinfection impacts the evolutionary fate of neutral and non-neutral variants in a simulated well-mixed phage population with constant, but limited, availability of host. We choose to focus on superinfection exclusion mechanisms that allow subsequent adsorption events, but prevent injection of subsequent DNA. This is so that the behaviour of phage grown in isolation will be unaffected by whether they are capable of preventing superinfection or not, thereby allowing us to make a more direct comparison between the (dis)advantages of the two strategies. We first quantify the effective population size of superinfecting (S) and superinfection-excluding (SX) populations to estimate how these strategies affect genetic drift. We then turn our attention to the effect of non-neutral mutations on (i) the phage growth rate in isolation and (ii) their ability to outcompete the wild-type. Having characterised both the neutral dynamics and the fitness of different variants, we put both aspects together to explore the balance between drift and selection in superinfecting and superinfection-excluding populations, showing that selection is consistently more efficient in superinfecting populations. Finally, we study the evolutionary fate of a mutation which changes whether an individual is capable of preventing superinfection or not. Overall, this work establishes a baseline expectation for how the simple occurrence of superinfection impacts fundamental evolutionary outcomes and provides insights into the selective pressure experienced by viral populations in limited, but constant host conditions.

Methods

Computational modelling framework

We study the evolutionary fate of phage mutants using a stochastic agent-based model. We simulate a well-mixed population of phages V interacting with a population of host bacteria that is kept at a constant density, similarly to a turbidostat[46,47]. Each phage has a defining set of life history parameters, namely an adsorption rate α, a lysis time τ and a burst size β, and each bacteria can either be in an uninfected B or an infected I state.

In each simulation timestep, adsorption, phage replication within the host and lysis occur. The number of infecting phage V_I in each step is drawn from a Poisson distribution whose mean corresponds to the expectated value $\alpha V(B+I)$ in a well-mixed population. The infecting phage are removed from the pool of free phage, and V_I bacteria, whether infected or uninfected, are chosen uniformly and with replacement to be the infection target. In both superinfecting and superinfection-excluding scenarios, the final burst size β and lysis time τ of the host are set by the first phage to infect it. This choice was made for the sake of simplicity, given the complex and varied nature of superinfection mechanisms[1,2]. In the case where multiple phage infect the same host in a single timestep, the 'first' phage is chosen randomly among those infecting the host. Phage replication within the host post-adsorption depends on whether superinfection is allowed or prevented:

Absence of superinfection: τ steps after the first adsorption event, the bacteria will lyse, releasing new phage into the pool of free phage. The number of phage released Y is drawn from a Poisson distribution with mean β.

Presence of superinfection: Pseudo-populations tracking the growth of phage inside the host are used (see Fig. 1b). During the intermediate steps between the first adsorption event and lysis, the total number of phage inside the host increases at a constant rate β/τ, determined by the initial infecting phage. These β/τ phages are allocated proportionally to each phage type inside the host at that time, in line with previous reports of a positive linear relationship between lysis time and burst size[48], and to reflect the intracellular competition for the host's resources. Because here we focus on the case of two superinfecting phage populations, this step-by-step allocation results in two pseudo-populations p_a and p_b. At the point of lysis, the total number of phage released Y is again drawn from a Poisson distribution with mean β. The number of phage released of one type Y_a is then drawn from a binomial distribution with Y attempts and probability $p_a/(p_a+p_b)$ of success, with any remaining phage being the other type ($Y_b = Y - Y_a$).

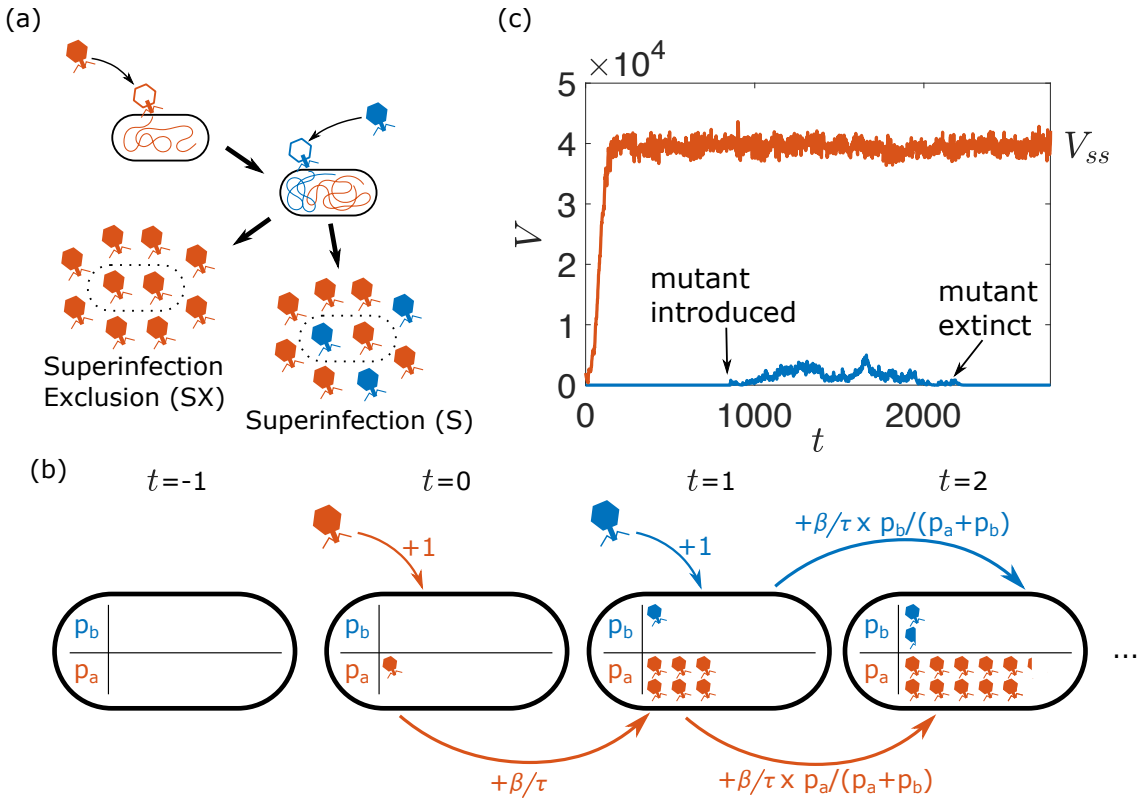

Figure 1. (a): In superinfection-excluding scenarios, all of the progeny released as the cell lyses are copies of the initial infecting phage, whereas when superinfecting in permitted, the progeny are split between both types of phage. (b): During superinfection, sudo-populations p_a and p_b are used to represent the growth of phage inside the host cells. These populations increase by 1 whenever a phage infects the host, and the total number of phage $(p_a + p_b)$ increases by β/τ in each time-step, with each population's increase being proportional to their relative size in the previous step. (c): An example realisation of the simulation. The resident phage population initially grows until it reaches a steady state, at which point a mutant phage is introduced to the population, and the simulation is run until extinction or fixation of the mutant.

Following lysis, the lysed bacteria are immediately replaced with a new, uninfected host, resulting in a bacterial population of constant size. We also introduce a decay, or removal, of free phage at rate δ, which accounts for natural phage decay and the outflow of the turbidostat system.

Simulations were initialised with B_0 uninfected bacteria and $2B_0$ "resident" phage, and then run until the phage, uninfected bacteria and infected bacteria populations each reached steady state values (V_{ss}, B_{ss} and I_{ss} respectively), as determined by their running average (Fig. 1c). This steady state arises due to a balance between phage production and loss and it is independent of the initial number of phages (Supporting Information, Fig. S1).

Measuring effective population size of the phage population

Consistent with previous work[49], we expect that the neutral standing diversity of the phage population, quantified by the heterozygosity H, will decay exponentially at long times due to genetic drift, so that $H(t) \propto e^{-2t/N_e}$ (Supporting Information), with the decay rate in units of generations being expressed in terms of an effective population size $2/N_e$ (Moran model[49]).

We track the viral heterozygosity H as a function of time, which in a biallelic viral population is given by

$$H = 2\langle f(1-f)\rangle, \tag{1}$$

where f and $(1-f)$ represent the frequencies of two neutral viral alleles in the population, and $\langle \dots \rangle$ indicates the average over independent simulations. $H(t)$ can be understood to be the time-dependent probability that two individuals chosen from the population are genetically distinct.

To determine the generation time T, we first calculate the *net reproduction rate* R_0, which represents the number of offspring an individual would be expected to produce if it passed through its lifetime conforming to the age-specific fertility and mortality

rates of the population at a given time (i.e. taking into account the fact that some individuals die before reproducing)[50]. R_0 can be calculated as

$$R_0 = \sum l_t m_t, \tag{2}$$

where l_t represents the proportion of individuals (in our case, phage) surviving to age t, and m_t represents the average number of offspring produced at age t.

There are two mechanisms in our simulations by which phages can 'die' when superinfection exclusion applies: either by decaying with rate δ, or by adsorbing to an infected host with rate αI_{ss}. In a sufficiently small timestep Δt, these rates correspond to a proportion $\delta\Delta t$ and $\alpha I_{ss}\Delta t$ of the total phage, respectively. Equivalently, these can be considered to be the probability that any single phage will die in the same period. As a result, the probability of a phage surviving to age t is $l_t = (1-\delta\Delta t - \alpha I_{ss}\Delta t)^{t/\Delta t}$.

The average number of offspring m_t produced at age t is 0 if $t < \tau$, because we assume that no phage is released before the lysis time. For $t > \tau$, m_t is given by the probability of successfully infecting a viable host in a timestep Δt, τ time earlier ($\alpha B_{ss}\Delta t$), multiplied by the yield of new phage ($\beta - 1$).

In the limit where $\Delta t \to 0$, this will result in a net reproductive rate of the form

$$R_0 = \lim_{\Delta t\to 0}\sum_{t=0}^{\infty} m_t l_t = \lim_{\Delta t\to 0}\sum_{t=\tau}^{\infty} \Delta t\,\alpha B_{ss}(\beta-1)(1-\Delta t(\delta+\alpha I_{ss}))^{t/\Delta t}, \tag{3}$$

$$= \int_{t=\tau}^{\infty} \alpha B_{ss}(\beta-1)e^{-(\delta+\alpha I_{ss})t}\,\mathrm{d}t, \tag{4}$$

$$= \frac{\alpha B_{ss}(\beta-1)}{\delta+\alpha I_{ss}} e^{-(\delta+\alpha I_{ss})\tau}, \tag{5}$$

where the integral starts at τ because no offspring are produced prior to that point.

Then the generation time T, defined as the average interval between the birth of an individual and the birth of its offspring, is

$$T = \lim_{\Delta t\to 0}\frac{\sum t l_t m_t}{R_0} = \frac{\int_{t=\tau}^{\infty} t\,\alpha B_{ss}(\beta-1)e^{-(\delta+\alpha I_{ss})t}\,\mathrm{d}t}{R_0} = \tau + \frac{1}{\delta+\alpha I_{ss}}. \tag{6}$$

Here, we will use resident phage parameters $\alpha = 3\times 10^{-6}$, $\tau = 15$, $\delta = 0.1$ and a total bacterial population of $B_0 = 1000$, which leads to $I_{ss} = 681$ and a generation time of $T = 24.8$. For comparison, coliphage T7 in liquid culture typically has parameters of $\tau \approx 10-20$ min, $\alpha \approx 10^{-9}$ ml/min and $B_0 \approx 10^6 - 10^8$ ml^{-1}, thereby yielding an $\alpha B_0 \approx 10^{-3} - 10^{-1}$ min^{-1}[51,52]. These values are comparable to our own if we equate 1 timestep = 1 min, and so $\tau = 15$ min, $\alpha B_0 = 3\times 10^{-3}$ min^{-1} and $T = 24.8$ min. This generation time is also supported by stochastic simulations of the phage adsorption and death processes (Supporting Information). Throughout this work, we use the same generation time for both superinfecting and superinfection-excluding populations (more details in the Supporting Information).

Measuring mutant fitness and growth rate

We start by defining a selective advantage s_{growth} in terms of the exponential growth rate r_{mut} of the mutant phage population relative to that of the resident phage r_{res}[53]:

$$s_{growth} = \frac{r_{mut}}{r_{res}} - 1. \tag{7}$$

The exponential growth rate is determined by simulating the growth of the corresponding phage population in isolation, and performing a linear fit to the log-transformed phage number as a function of time, which is then averaged over 500 independent simulations. It should be noted that as there is only one type of phage in these simulations, the growth rate of both superinfecting and superinfection-excluding populations is the same.

We also characterised the fitness of mutants in a competitive setting, by simulating a resident population until steady state, and then replacing 50% of the population with the mutant. In this direct competition scenario, we determine the selective (dis)advantage s_{comp} of the mutant phage by tracking the relative growth of mutant and resident populations, so that

$$\frac{V_{mut}}{V_{res}} = \frac{V_{mut}(t=0)e^{r_{res}(1+s_{comp})t}}{V_{res}(t=0)e^{r_{res}t}} = e^{r_{res}s_{comp}t}, \tag{8}$$

as $V_{mut}(t=0) = V_{res}(t=0)$. s_{comp} is determined from the average of 200 simulations. Importantly, in contrast to s_{growth}, this competitive selective advantage (s_{comp}) can in principle differ between superinfecting (s_S) and superinfection-excluding (s_{SX}) phage populations. In the absence of any interactions between the two competing phage populations, s_{growth} and s_{comp} are typically expected to be the same.

Measuring mutant probability of fixation

To measure fixation probabilities of individual mutations, we allow our simulations to reach steady state, we then introduce a single mutant phage into the free phage population, and run the simulation until either fixation or extinction occurs. This process is repeated at least 14 million times for each set of parameters. The probability of mutant fixation P_{fix} is determined from the fraction of simulations where the mutant fixed, n_{fix}, over the total number of simulations run, n (i.e. $P_{fix} = n_{fix}/n$). Assuming a binomial distribution, the error in our estimate of the fixation probability ΔP_{fix} is given by $\Delta P_{fix} = \sqrt{n_{fix}}/n$.

Results

Superinfection leads to a larger effective population size

First, we find that genetic diversity consistently declines faster in populations that prevent superinfection, indicating a smaller effective population size when compared to superinfecting populations. This can be intuitively understood by considering that in the superinfecting scenario, each phage has more opportunity to successfully infect a host cell, since secondary infections can result in the production of some offspring when the cell lyses. Therefore, more phage are able to contribute to the next generation, thereby slowing down diversity loss.

In addition, Fig. 2 shows that in both superinfecting and superinfection-excluding populations higher adsorption rate and burst size, and shorter lysis time result in larger effective populations. This observation is, however, partially attributable to the change in total phage population $N_T = (V_{ss} + \beta I_{ss})$, where V_{ss} indicates the steady state free phage population, I_{ss} indicates the steady state number of infected bacteria, and so βI_{ss} represents the number of phage that inevitably will join the free phage population.

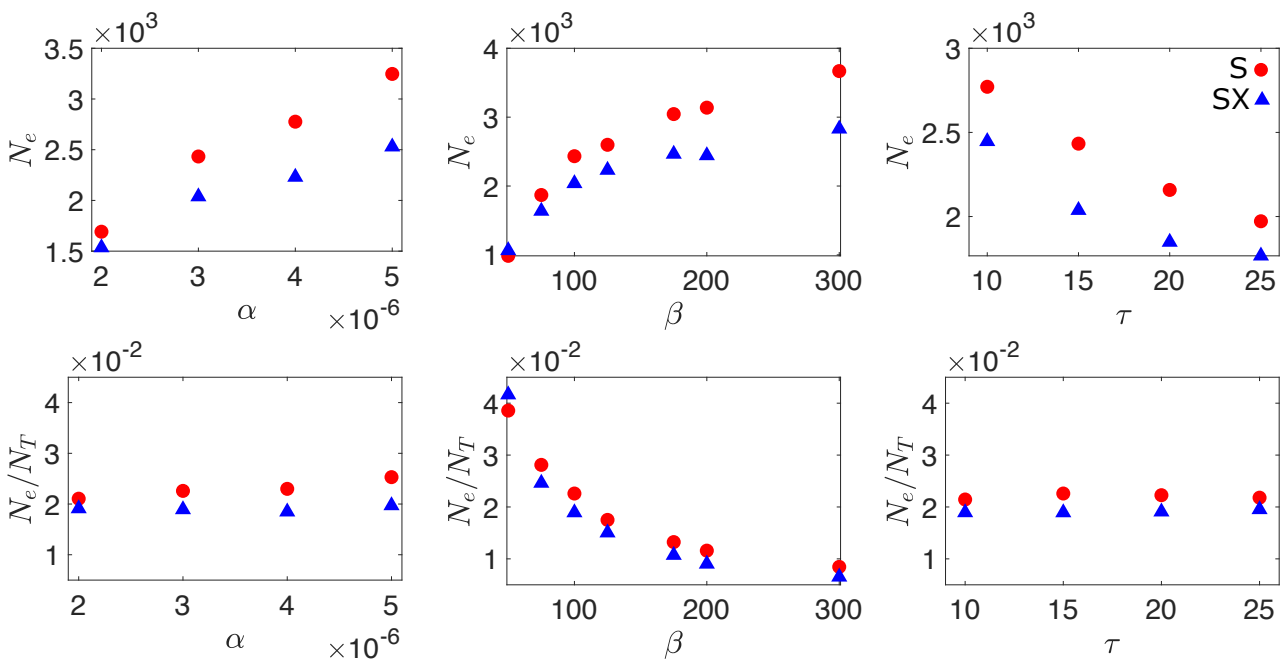

Figure 2. The effective population size in both superinfecting (S) and superinfection-excluding (SX) populations as a function of adsorption rate α, burst size β and lysis time τ. Effective population size are also shown scaled by the size of the total phage population $N_T = (V_{ss} + \beta I_{ss})$. Parameters used were $\alpha = 3 \times 10^{-6}$, $\beta = 100$ and $\tau = 15$ unless otherwise stated. Throughout, $\delta = 0.1$ and $B_0 = 1000$.

Indeed, adsorption rate and lysis time impact both the effective and actual population sizes in the same way (i.e. $N_e/N_T \approx$ const.). By contrast, larger burst sizes increase the effective population size less than the actual population size (Fig. 2), resulting in a decrease of N_e/N_T. This can be interpreted by noticing that while increasing burst size results in more phage, the number of phage that can actually contribute to the next generation (i.e. the effective population size) is limited by the number of bacteria that are available. Therefore, as burst size is increased, a larger fraction of phage become wasted.

Neutral mutants are consistently more likely to fix in superinfecting populations

To continue our characterisation of the neutral dynamics in both superinfecting and superinfection-excluding populations, we turn to the fixation probabilities of neutral mutants, and determine how they depend on the phage infection parameters.

Because the total phage population size depends on the life history parameters, the initial mutant frequency corresponding to one mutant phage inoculated in the population also varies with life history parameters. To account for this effect, we rescale the fixation probability by the initial frequency of the mutant $f_0^* = 1/(V_{ss} + \beta I_{ss})$, which is the same in superinfecting and superinfection-excluding populations. Fig. 3 shows that $P_{fix}/f_0^* \approx 1$ as the parameters are varied, indicating that the total number of phages for a given set of parameters is the main controller of neutral dynamics. Indeed, we find that the impact of the life history parameters on the probability of fixation is what one would intuitively expect (Supporting Information, Fig. S6): larger adsorption rate and burst size, and shorter lysis time, increase the steady-state size of the phage population, and reduce P_{fix}. By describing the average behaviour of our simulations with a system of ordinary differential equations (ODEs), we confirm that the ODE solution for the total phage population at steady-state N_T is the same as in the stochastic model (Supporting Information, Fig. S6).

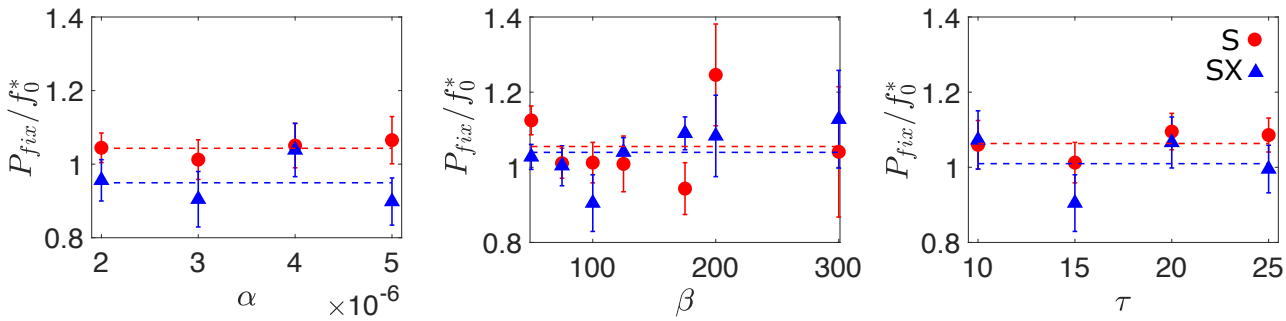

Figure 3. Probability of mutant fixation P_{fix} in the superinfecting (S) and non superinfection exclusing (SX) scenarios, scaled by the initial frequency of the mutant $f_0^* = 1/(V_{ss} + \beta I_{ss})$, as a function of adsorption rate α, burst size β and lysis time τ. Dashed lines indicate the simple average of the data for both the superinfecting (blue) and superinfection-excluding (red) scenarios. These lines indicate that neutral mutants in superinfecting populations experience a small advantage over mutants in an equivalent superinfection-excluding population. Unscaled P_{fix} data can be seen in Supporting Information, Fig. S6. Unless otherwise stated, the parameters used were $\alpha = 3 \times 10^{-6}$, $\beta = 100$, $\tau = 15$, $\delta = 0.1$ and $B_0 = 1000$.

Fig. 3 also shows that, on average, neutral mutants in the superinfecting scenario are more likely to fix than mutants in an equivalent superinfection-excluding population (blue and red dashed lines in Fig. 3 respectively). This result agrees with that found by Wodarz *et al.*[45], who showed that in a superinfecting viral population, higher multiplicities of infection slightly favoured rare neutral and disadvantageous mutants in the short term. The intuition behind this observation is that in the period shortly after the introduction of a mutant, in the superinfecting scenario, the mutant can increase in number by adsorbing to both uninfected and infected cells. By contrast, the resident phage can only increase in number by adsorbing to uninfected cells, because at this stage all infected cells are already infected with resident phage. As a result, superinfection increases the mutant's chance of survival in the early stages in comparison to the superinfection-excluding counterpart, similarly to conditions of high vs. low MOI[45].

Higher growth rate does not translate into competitive advantage

To investigate the evolutionary fate of non-neutral mutations, we first characterise how phage growth rate and competitive fitness is affected by changes to the phage life history parameters, i.e., adsorption rate α, burst size β and the lysis time τ, relative to the values used in our neutral simulations (Fig. 3).

Fig. S7 shows that increasing burst size or adsorption rate results in a larger selective advantage s both in isolation and in direct competition. However, while variations in burst size affect similarly the phage growth rate in isolation and its (dis)advantage in a competitive setting ($s_{growth} \approx s_{comp}$, Fig. 4), variations in adsorption rate lead to a stronger competitive (dis)advantage than what would be predicted by the growth rate ($|s_{growth}| < |s_{comp}|$). The intuition behind this result is that increasing adsorption rate becomes particularly advantageous in a competitive environment, as being the *first* virus to infect a host allows the virus to have largely (superinfection scenario) or completely (superinfection exclusion scenario) exclusive access to the host resources.

The impact of altering lysis time τ is surprising. Fig. S7 shows that increasing τ results in a reduced growth rate, as intuition suggests. Yet, no discernible impact on s_{comp} is observed (Fig. 4). This result is supported by our ODE model (Supporting Information), which shows that once the system is at steady-state, alterations to lysis time offer no advantage to one phage over the other (Fig. S8). We believe that this is a special feature of a turbidostat setting, as lysed hosts are immediately replaced by uninfected cells, providing the same number of viable hosts independently of the time needed by the phage to lyse them.

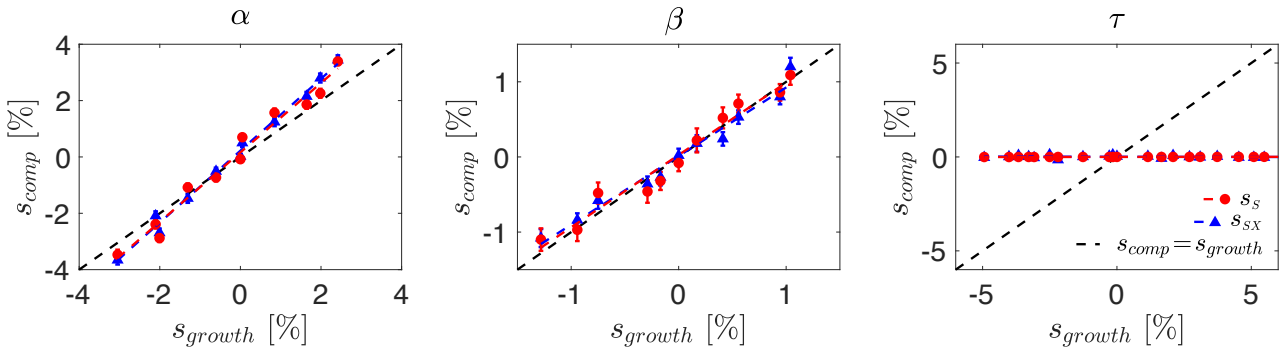

Figure 4. The selective advantage in a competitive setting s_{comp} as a function of the change in growth rate s_{growth}, when changing adsorption rate α, burst size β and lysis time τ. Resident parameters used were $\alpha = 3 \times 10^{-6}$, $\beta = 100$ and $\tau = 15$. As before $\delta = 0.1$ and $B_0 = 1000$. Error bars on x axis have been omitted for clarity.

Superinfection results in more efficient selection

Having characterised how changes to the phage infection parameters alter first genetic drift and second fitness, we now put both ingredients together and investigate the dynamics of non-neutral mutants. To this end, we simulate a resident phage population to steady state, introduce a single non-neutral mutant and then run the simulation until extinction or fixation occurs.

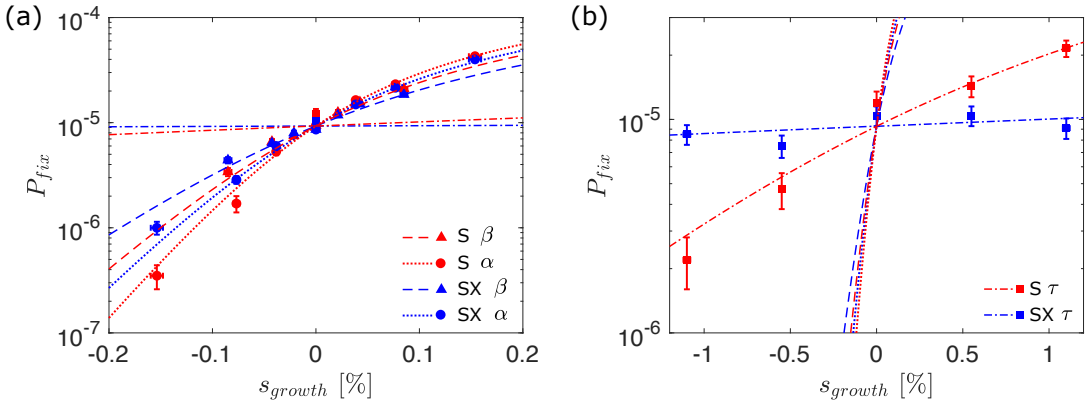

Figure 5. Probability of mutant fixation P_{fix} as a function of selective growth advantage s_{growth}. Points indicate simulation results, while lines, for (a) α and β indicate theoretically predicted values in a Moran model with equivalent parameters (Eq. 9). Lines for (b) τ show an optimised fit to the Moran model, with $s = \sigma s_{growth}$, as we were unable to measure the relationship between s_{growth} and s_{comp} (see Fig. 4). We find $\sigma_{SX} = 0.008$ and $\sigma_S = 0.075$.

In agreement with our observations regarding the difference between growth rate and competitive fitness, we find that the value of s_{growth} is not sufficient to determine the fixation probability of the corresponding mutant (Fig. 5): a mutation associated with a higher adsorption rate α increases the mutant's chance to fix more than a mutation which alters the burst size β and leads to the same growth rate. We also find that beneficial mutations are consistently more likely to fix (and deleterious mutations more likely to go extinct) in superinfecting populations (red) than superinfection-excluding populations (blue). This suggests that superinfection improves selection efficiency, by more readily fixing beneficial mutations and purging deleterious ones.

To provide a theoretical framework to our findings, we compare the simulation data to the fixation probabilities one would expect in a corresponding Moran model. For small selective advantage s, the probability of fixation is given by

$$P_{fix} = \frac{1 - e^{-N_e s f_0}}{1 - e^{-N_e s}}, \tag{9}$$

where f_0 is the initial frequency of the mutant in the population with effective population size N_e[49,54]. Our earlier results on neutral dynamics and fitness provide independent measurements of the parameters in Eq. 9 for different values of α and β: $f_0 = f_0^*$ from our initial condition (i.e., $1/N_T$, where N_T is the steady-state phage population size when the mutant is introduced); N_e is measured from the decay of heterozygosity (Fig. 2); and $s = s_{comp}(s_{growth})$ is derived from our measurements

of the relationship between competitive and growth rate advantage (Fig. 4). These theoretical predictions are plotted without additional fitting parameters as lines in Fig. 5. For mutations in τ, we were unable to measure the relationship between s_{growth} and s_{comp} ($s_{comp} \approx 0$, Fig. 4), and so here we use a fitting parameter σ such that $s_{comp} = \sigma s_{growth}$. We find $\sigma_{SX} = 0.008$ and $\sigma_S = 0.075$.

Fig. 5 shows that the theoretical prediction from the appropriately parameterised Moran model matches the simulation data remarkably well, despite the complex internal infection dynamic (see Supporting Information for quantitative comparison). We do note however that the simulation data consistently do not meet at the same point when $s = 0$ in the superinfecting scenario. This is because of the effect outlined in Fig. 3, where rare mutants initially experience a slight advantage in the superinfecting scenario because they are able to increase in number by infecting both uninfected and infected cells. To test the validity of our findings across parameter space, we also perform all of the above analysis with different resident parameters, obtaining the same results (Supporting Information).

Superinfection exclusion slows down adaptability in the long run, but is a winning strategy in the short term

Our findings imply that, even in the absence of intra-cellular processes such as recombination, superinfection results in more efficient selection, so that beneficial mutations are relatively more likely to fix, and deleterious ones are more likely to be purged, leading to a fitter overall population in the long run. From the point of view of viral adaptation, allowing superinfection ultimately seems like the better long-term strategy. It is therefore puzzling why several natural phage populations have developed sophisticated mechanisms to prevent superinfection, particularly given that employing these mechanisms is expected to come with a biological cost, such as reduced burst size[55,56] or increased lysis time[57].

To address this question, we consider the fate of mutations that either (i) remove the mutant's ability to prevent superinfection in a resident superinfection-excluding population or (ii) provide the mutant the ability to prevent superinfection in a resident superinfecting population. Fig. 6 shows that if the mutant is neutral ($\beta_{mut} = \beta_{res} = 100$), then the superinfection-excluding mutant is two orders of magnitude more likely to fix than the expectation based on its initial frequency f_0^*, and that, by contrast, the superinfecting mutant is at least two orders of magnitude more likely to go extinct (we actually find no instances of mutant fixation, but our detection power is limited by the number of simulation runs, so the value should be interpreted as a lower bound). This indicates that mutants which are able to prevent superinfection experience a very strong selective advantage over their superinfecting counterparts, and vice-versa.

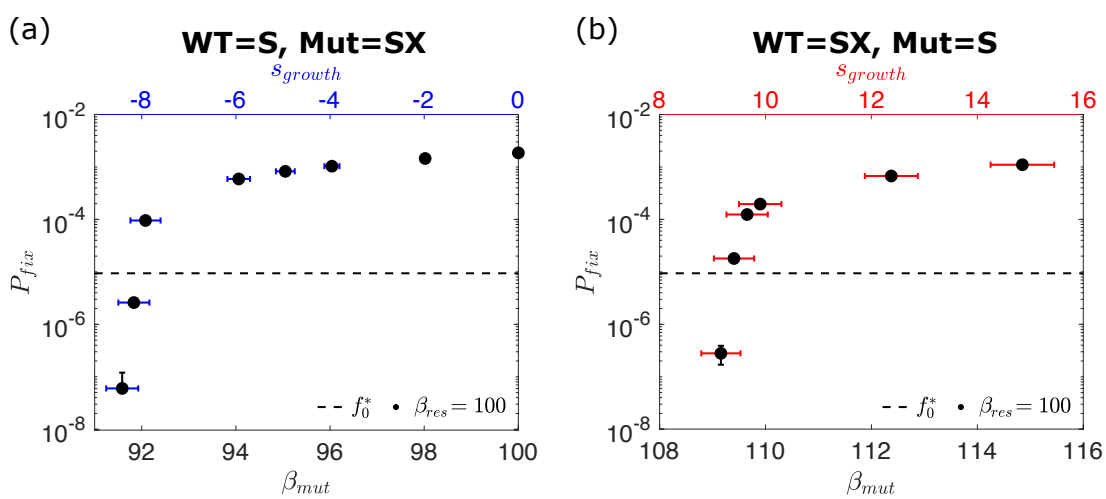

Figure 6. (a) The probability P_{fix} of a mutant which prevents superinfection fixing in a population that allows it, as a function of mutant burst size β_{mut}. (b) The probability P_{fix} of a mutant which allows superinfection fixing in a population that prevents it, as a function of mutant burst size β_{mut}. It can be seen that the superinfecting mutant requires a significantly increased burst size to fix, and conversely the superinfection-excluding mutant can fix, even if its burst size is greatly reduced.

To account for the possibility that superinfection exclusion comes at a cost in phage growth, as preventing superinfection likely requires the production of extra proteins, the resources for which could otherwise have gone to the production of more phage, we consider the case where superinfection exclusion is associated with a reduction in burst size[55]. Remarkably, we find that even when preventing superinfection carries a burden of 8% reduction in burst size ($s_{growth} < -8\%$), the superinfection-excluding mutant still fixes more often than a neutral superinfecting mutant (Fig. 6). Conversely, a minimum of 9% increase in burst size ($s_{growth} > 9\%$) is necessary to give a superinfecting mutant any chance of fixing in a superinfection-excluding

population. This indicates that while allowing superinfection increases selection efficiency at the population level, preventing it is ultimately a winning strategy in the short term, partially explaining why superinfection exclusion is so common in nature[3,4].

Discussion

In this work, we have considered the impact of either allowing or preventing superinfection on the evolution of viral populations. Using a stochastic agent-based model of viral infection, we have shown that allowing superinfection reduces the strength of genetic drift, leading to an increase in effective population size. Weaker fluctuations result in a higher efficiency of selection in viral populations, with beneficial mutations fixing more frequently, and deleterious ones more readily being purged from the population. Despite the long term, population-wide benefit of allowing superinfection, we find that if a mutant arises which is capable of preventing superinfection, it will fix remarkably easily, even if its growth rate is heavily compromised. Conversely, if the whole population is capable of preventing superinfection, mutants which allow it will have almost no chance of ever succeeding.

The evolutionary impact of superinfection has most often focussed on the role of intracellular interactions and competition[9–16], such as genetic recombination and reassortment[17–20], and viral complementation[20–24]. A prevalent finding (amongst others) is that recombination and reassortment can improve the efficiency of selection in viral populations which do not exclude superinfection. Remarkably, our work demonstrates that the basic occurrence of superinfection alone, absent of any recombination or reassortment, is capable of increasing the selection efficiency. In this context, our results provide a useful baseline for comparison when trying to assess the significance of each of these more complex effects, which may or may not be present in different situations.

An unexpected finding of this work is that in the turbidostat system we consider, while increased adsorption rate and burst size both increase the fitness of the phage population in all respects, lysis time does not play a role in the competitive dis(advantage) experienced once the system has reached a steady-state. This result is somewhat in contrast with previous studies showing that in well-mixed liquid cultures where there is an abundant supply of hosts, generally higher adsorption rates and lower lysis times result in an increase in phage fitness[48,52,58,59]. The key difference between such liquid culture and the turbidostat system we model here is that in the former host cells are not maintained at a constant density, but the phage population continues to grow until no bacteria remain. This finding illustrates how the presence or absence of a co-existing steady-state between phage and bacteria completely alters the selective pressure on the phage with important implications for studies into the co-evolution of phage and bacteria populations using continuous culturing set-ups[60–62]. In particular, our results suggests that in an evolutionary experiment in a turbidostat, the virus should evolve towards very large burst size even if this feature comes at the cost of longer lysis times[52].

The differing strategies of allowing or preventing superinfection can be viewed in the context of the Prisoner's Dilemma, analogously to the experimental work on RNA phage $\phi 6$ presented in[26,27]. In our work, phage can either allow or prevent superinfection, which in the context of the Prisoner's Dilemma can be interpreted as either 'co-operating', by sharing the host's resources, or 'defecting', by acting selfishly and keeping all of the host's resources to oneself, respectively. Overall the 'best' outcome occurs when all individuals co-operate, because allowing superinfection increases the efficiency of selection, making it easier to fix beneficial mutations and purge deleterious ones, in the long run increasing the fitness of the population. However, analogous to the Prisoner's Dilemma, in a population of co-operators a mutant phage can gain a significant reward by defecting (preventing superinfection), as it greatly increases its chances of fixation. Conversely, in a population of defectors, a mutant co-operator is severely punished as it has a very low probability of fixation, and so in this situation it is also in the interest of the mutant to be a defector. Therefore, as in the Prisoner's Dilemma, while mutual co-operation yields overall the best outcome, defection is the *dominant strategy*, because it always results in a better outcome regardless of the other side's strategy.

Following this, it is natural to wonder how the (dis)advantages and impact of either strategy depends on the selective pressure experienced in different environments. The relationship between viral fitness and the phage life-history parameters (adsorption rate, lysis time and burst size) has been shown to be very context-dependent in both well-mixed and spatially structured settings. For instance, as noted previously, well-mixed settings generally favour higher adsorption rates[63], but in spatially structured settings phage with lower adsorption rates are more successful[64,65]. Additionally, it has been shown previously that eco-evolutionary feedbacks at the edge of expanding viral populations can result in travelling waves with vastly different effective population size[66]. Given that competition for resources (i.e. viable hosts) in spatially structured environments is local rather than global, phage are more likely to be in competition with other genetically identical phage released by nearby cells. It is therefore possible that superinfection exclusion proves less useful in this context than in well-mixed environments where competition is global and phage are more likely to encounter other genetically different viruses. All of this points at the role of superinfection strategies and other social viral behaviour on the eco-evolutionary dynamics of spatially expanding viral populations as an exciting avenue for future research.

Acknowledgements

MH acknowledges studentship funding from EPSRC under grant number EP/R513180/1. This work was performed using resources provided by the Cambridge Service for Data Driven Discovery (CSD3) operated by the University of Cambridge Research Computing Service, provided by Dell EMC and Intel using Tier-2 funding from the Engineering and Physical Sciences Research Council (capital grant EP/P020259/1), and DiRAC funding from the Science and Technology Facilities Council.

References

1. Roux, S., Hallam, S. J., Woyke, T. & Sullivan, M. B. Viral dark matter and virus–host interactions resolved from publicly available microbial genomes. *eLife* **4**, DOI: 10.7554/eLife.08490.001 (2015).
2. Díaz-Muñoz, S. L. Viral coinfection is shaped by host ecology and virus-virus interactions across diverse microbial taxa and environments. *Virus Evol.* **3**, DOI: 10.1093/ve/vex011 (2017).
3. Labrie, S. J., Samson, J. E. & Moineau, S. Bacteriophage resistance mechanisms. *Nat. Rev. Microbiol.* **8**, 317–327, DOI: 10.1038/nrmicro2315 (2010).
4. van Houte, S., Buckling, A. & Westra, E. R. Evolutionary Ecology of Prokaryotic Immune Mechanisms. *Microbiol. molecular biology reviews : MMBR* **80**, 745–63, DOI: 10.1128/MMBR.00011-16 (2016).
5. Braun, V., Killmann, H. & Herrmann, C. Inactivation of FhuA at the cell surface of Escherichia coli K-12 by a phage T5 lipoprotein at the periplasmic face of the outer membrane. *J. Bacteriol.* **176**, 4710–4717, DOI: 10.1128/jb.176.15.4710-4717.1994 (1994).
6. Pedruzzi, I., Rosenbusch, J. P. & Locher, K. P. Inactivation in vitro of the Escherichia coli outer membrane protein FhuA by a phage T5-encoded lipoprotein. *FEMS Microbiol. Lett.* **168**, 119–125, DOI: 10.1111/j.1574-6968.1998.tb13264.x (1998).
7. Lu, M. J., Stierhof, Y. D. & Henning, U. Location and unusual membrane topology of the immunity protein of the Escherichia coli phage T4. *J. Virol.* **67** (1993).
8. Lu, M. J. & Henning, U. Superinfection exclusion by T-even-type coliphages. *Trends Microbiol.* **2**, 137–139, DOI: 10.1016/0966-842X(94)90601-7 (1994).
9. Frank, S. A. All of life is social, DOI: 10.1016/j.cub.2007.06.005 (2007).
10. Weitz, J. S., Mileyko, Y., Joh, R. I. & Voit, E. O. Collective decision making in bacterial viruses. *Biophys. J.* **95**, 2673–2680, DOI: 10.1529/biophysj.108.133694 (2008).
11. Refardt, D. Within-host competition determines reproductive success of temperate bacteriophages. *ISME J.* **5**, 1451–1460, DOI: 10.1038/ismej.2011.30 (2011).
12. Ojosnegros, S., Perales, C., Mas, A. & Domingo, E. Quasispecies as a matter of fact: Viruses and beyond, DOI: 10.1016/j.virusres.2011.09.018 (2011).
13. Koelle, K., Farrell, A. P., Brooke, C. B. & Ke, R. Within-host infectious disease models accommodating cellular coinfection, with an application to influenza†. *Virus Evol.* **5**, 18, DOI: 10.1093/ve/vez018 (2019).
14. Iranzo, J., Faure, G., Wolf, Y. I. & Koonin, E. V. Game-Theoretical Modeling of Interviral Conflicts Mediated by Mini-CRISPR Arrays. *Front. Microbiol.* **11**, 381, DOI: 10.3389/fmicb.2020.00381 (2020).
15. Vafadar, S., Shahdoust, M., Kalirad, A., Zakeri, P. & Sadeghi, M. Competitive exclusion during co-infection as a strategy to prevent the spread of a virus: A computational perspective. *PLOS ONE* **16**, e0247200, DOI: 10.1371/journal.pone.0247200 (2021).
16. Sanjuán, R. & Domingo-Calap, P. Genetic Diversity and Evolution of Viral Populations. In *Encyclopedia of Virology*, 53–61, DOI: 10.1016/b978-0-12-809633-8.20958-8 (Elsevier, 2021).
17. Bretscher, M. T., Althaus, C. L., Müller, V. & Bonhoeffer, S. Recombination in HIV and the evolution of drug resistance: for better or for worse? *BioEssays* **26**, 180–188, DOI: 10.1002/bies.10386 (2004).
18. Vijay, N. N., Vasantika, Ajmani, R., Perelson, A. S. & Dixit, N. M. Recombination increases human immunodeficiency virus fitness, but not necessarily diversity. *J. Gen. Virol.* **89**, 1467–1477, DOI: 10.1099/vir.0.83668-0 (2008).
19. Weller, S. K. & Sawitzke, J. A. Recombination Promoted by DNA Viruses: Phage λ to Herpes Simplex Virus. *Annu. Rev. Microbiol.* **68**, 237–258, DOI: 10.1146/annurev-micro-091313-103424 (2014).
20. Gao, H. & Feldman, M. W. Complementation and epistasis in viral coinfection dynamics. *Genetics* **182**, 251–263, DOI: 10.1534/genetics.108.099796 (2009).

21. Froissart, R. *et al.* Co-infection Weakens Selection Against Epistatic Mutations in RNA Viruses. *Genetics* **168**, 9–19, DOI: 10.1534/genetics.104.030205 (2004).

22. García-Arriaza, J., Manrubia, S. C., Toja, M., Domingo, E. & Escarmís, C. Evolutionary Transition toward Defective RNAs That Are Infectious by Complementation. *J. Virol.* **78**, 11678–11685, DOI: 10.1128/jvi.78.21.11678-11685.2004 (2004).

23. García-Arriaza, J., Ojosnegros, S., Dávila, M., Domingo, E. & Escarmís, C. Dynamics of Mutation and Recombination in a Replicating Population of Complementing, Defective Viral Genomes. *J. Mol. Biol.* **360**, 558–572, DOI: 10.1016/j.jmb.2006.05.027 (2006).

24. Gelderblom, H. C. *et al.* Viral complementation allows HIV-1 replication without integration. *Retrovirology* **5**, 60, DOI: 10.1186/1742-4690-5-60 (2008).

25. Turner, P. E. & Chao, L. Sex and the Evolution of Intrahost Competition in RNA Virus $\phi 6$. *Genetics* **150**, 523–532, DOI: 10.1093/genetics/150.2.523 (1998).

26. Turner, P. E. & Chao, L. Prisoner's dilemma in an RNA virus. *Nature* **398**, 441–443, DOI: 10.1038/18913 (1999).

27. Turner, P. E. & Chao, L. Escape from prisoner's dilemma in RNA phage $\phi 6$. *Am. Nat.* **161**, 497–505, DOI: 10.1086/367880 (2003).

28. Dennehy, J. J., Duffy, S., O'Keefe, K. J., Edwards, S. V. & Turner, P. E. Frequent Coinfection Reduces RNA Virus Population Genetic Diversity. *J. Hered.* **104**, 704–712, DOI: 10.1093/jhered/est038 (2013).

29. Donahue, D. A., Bastarache, S. M., Sloan, R. D. & Wainberg, M. A. Latent HIV-1 Can Be Reactivated by Cellular Superinfection in a Tat-Dependent Manner, Which Can Lead to the Emergence of Multidrug-Resistant Recombinant Viruses. *J. Virol.* **87**, 9620–9632, DOI: 10.1128/jvi.01165-13 (2013).

30. Chao, L. Evolution of sex in RNA viruses, DOI: 10.1016/0169-5347(92)90207-R (1992).

31. Asatryan, A., Wodarz, D. & Komarova, N. L. New virus dynamics in the presence of multiple infection. *J. Theor. Biol.* **377**, 98–109, DOI: 10.1016/j.jtbi.2015.04.014 (2015).

32. Dixit, N. M. & Perelson, A. S. Multiplicity of Human Immunodeficiency Virus Infections in Lymphoid Tissue. *J. Virol.* **78**, 8942–8945, DOI: 10.1128/jvi.78.16.8942-8945.2004 (2004).

33. Dixit, N. M. & Perelson, A. S. HIV dynamics with multiple infections of target cells. *Proc. Natl. Acad. Sci. United States Am.* **102**, 8198–8203, DOI: 10.1073/pnas.0407498102 (2005).

34. Althaus, C. L. & Bonhoeffer, S. Stochastic Interplay between Mutation and Recombination during the Acquisition of Drug Resistance Mutations in Human Immunodeficiency Virus Type 1. *J. Virol.* **79**, 13572–13578, DOI: 10.1128/jvi.79.21.13572-13578.2005 (2005).

35. Fraser, C. HIV recombination: What is the impact on antiretroviral therapy? *J. Royal Soc. Interface* **2**, 489–503, DOI: 10.1098/rsif.2005.0064 (2005).

36. Wodarz, D. & Levy, D. N. Effect of different modes of viral spread on the dynamics of multiply infected cells in human immunodeficiency virus infection. *J. Royal Soc. Interface* **8**, 289–300, DOI: 10.1098/rsif.2010.0266 (2011).

37. Cummings, K. W., Levy, D. N. & Wodarz, D. Increased burst size in multiply infected cells can alter basic virus dynamics. *Biol. Direct* **7**, 16, DOI: 10.1186/1745-6150-7-16 (2012).

38. May, R. M. & Nowak, M. A. Superinfection, metapopulation dynamics, and the evolution of diversity. *J. Theor. Biol.* **170**, 95–114, DOI: 10.1006/jtbi.1994.1171 (1994).

39. Nowak, M. A. & May, R. M. Superinfection and the evolution of parasite virulence. *Proc. Royal Soc. B: Biol. Sci.* **255**, 81–89, DOI: 10.1098/rspb.1994.0012 (1994).

40. Van Baalen, M. & Sabelis, M. W. The dynamics of multiple infection and the evolution of virulence. *Am. Nat.* **146**, 881–910, DOI: 10.1086/285830 (1995).

41. Alizon, S. & Van Baalen, M. Multiple infections, immune dynamics, and the evolution of virulence. *Am. Nat.* **172**, 150–168, DOI: 10.1086/590958 (2008).

42. Alizon, S., de Roode, J. C. & Michalakis, Y. Multiple infections and the evolution of virulence. *Ecol. Lett.* **16**, 556–567, DOI: 10.1111/ele.12076 (2013).

43. Leeks, A., Segredo-Otero, E. A., Sanjuán, R. & West, S. A. Beneficial coinfection can promote within-host viral diversity. *Virus Evol.* **4**, DOI: 10.1093/ve/vey028 (2018).

44. Phan, D. & Wodarz, D. Modeling multiple infection of cells by viruses: Challenges and insights. *Math. Biosci.* **264**, 21–28, DOI: https://doi.org/10.1016/j.mbs.2015.03.001 (2015).

45. Wodarz, D., Levy, D. N. & Komarova, N. L. Multiple infection of cells changes the dynamics of basic viral evolutionary processes. *Evol. Lett.* **3**, 104–115, DOI: 10.1002/evl3.95 (2019).

46. Bryson, V. & Szybalski, W. Microbial selection, DOI: 10.1126/science.116.3003.45 (1952).

47. Gresham, D. & Dunham, M. J. The enduring utility of continuous culturing in experimental evolution. *Genomics* **104**, 399–405, DOI: 10.1016/j.ygeno.2014.09.015 (2014).

48. Wang, I.-N. Lysis Timing and Bacteriophage Fitness. *Genetics* **172**, 17–26 (2006).

49. Moran, P. A. Random processes in genetics. *Math. Proc. Camb. Philos. Soc.* **54**, 60–71, DOI: 10.1017/S0305004100033193 (1958).

50. Preston, S., Heuveline, P. & Guillot, M. *Demography: Measuring and Modeling Population Processes*. Demography: Measuring and Modeling Population Processes (Wiley, 2000).

51. Fort, J. & Méndez, V. Time-delayed spread of viruses in growing plaques. *Phys. Rev. Lett.* **89**, DOI: 10.1103/PhysRevLett.89.178101 (2002).

52. Heineman, R. H. & Bull, J. J. Testing optimality with experimental evolution: lysis time in a bacteriophage. *Evol. international journal organic evolution* **61**, 1695–709, DOI: 10.1111/j.1558-5646.2007.00132.x (2007).

53. Fisher, R. A. & Bennett, J. H. *The Genetical Theory of Natural Selection: A Complete Variorum Edition* (OUP Oxford, 1999).

54. Dinh, K. N., Corey, S. J. & Kimmel, M. Application of the Moran Model in Estimating Selection Coefficient of Mutated CSF3R Clones in the Evolution of Severe Congenital Neutropenia to Myeloid Neoplasia. *Front. Physiol.* **11**, 806, DOI: 10.3389/fphys.2020.00806 (2020).

55. Delbrück, M. Interference between bacterial viruses; the mutual exclusion effect and the depressor effect. *J. bacteriology* **50**, 151–170 (1945).

56. Karam, J. D., Drake, J. W., Kreuzer, K. N., Hall, D. H. & Mosig, G. *Molecular Biology of Bacteriophage T4* (American Society for Microbiology, 1994).

57. Abedon, S. T. Lysis of lysis-inhibited bacteriophage T4-infected cells. *J. Bacteriol.* **174**, 8073–8080, DOI: 10.1128/jb.174.24.8073-8080.1992 (1992).

58. Wang, I. N., Dykhuizen, D. E. & Slobodkin, L. B. The evolution of phage lysis timing. *Evol. Ecol.* **10**, 545–558, DOI: 10.1007/BF01237884 (1996).

59. Shao, Y. & Wang, I. N. Bacteriophage adsorption rate and optimal lysis time. *Genetics* **180**, 471–482, DOI: 10.1534/genetics.108.090100 (2008).

60. Spanakis, E. & Horne, M. T. Co-adaptation of Escherichia coli and coliphage γvir in continuous culture. *J. Gen. Microbiol.* **133**, 353–360, DOI: 10.1099/00221287-133-2-353 (1987).

61. Mizoguchi, K. *et al.* Coevolution of bacteriophage PP01 and Escherichia coli O157:H7 in continuous culture. *Appl. Environ. Microbiol.* **69**, 170–176, DOI: 10.1128/AEM.69.1.170-176.2003 (2003).

62. Koskella, B. & Brockhurst, M. A. Bacteria-phage coevolution as a driver of ecological and evolutionary processes in microbial communities. *FEMS Microbiol. Rev.* **38**, 916–931, DOI: 10.1111/1574-6976.12072 (2014).

63. Bull, J. J., Heineman, R. H. & Wilke, C. O. The phenotype-fitness map in experimental evolution of phages. *PLoS ONE* **6**, 27796, DOI: 10.1371/journal.pone.0027796 (2011).

64. Kerr, B., Neuhauser, C., Bohannan, B. J. M. & Dean, A. M. Local migration promotes competitive restraint in a host-pathogen 'tragedy of the commons'. *Nature* **442**, 75–78, DOI: 10.1038/nature04864 (2006).

65. Roychoudhury, P., Shrestha, N., Wiss, V. R. & Krone, S. M. Fitness benefits of low infectivity in a spatially structured population of bacteriophages. *Proc. The Royal Soc. B: Biol. Sci.* **281**, DOI: 10.1098/rspb.2013.2563 (2014).

66. Hunter, M., Krishnan, N., Liu, T., Möbius, W. & Fusco, D. Virus-Host Interactions Shape Viral Dispersal Giving Rise to Distinct Classes of Traveling Waves in Spatial Expansions. *Phys. Rev. X* **11**, 21066, DOI: 10.1103/PhysRevX.11.021066 (2021).

Supporting Information

This Supporting Information (SI) contains expanded data analysis and outlines an ordinary differential equation (ODE) model which describes the average behaviour of our system.

Contents

1 Steady-States Are Independent of Initial Conditions **1**

2 Effective Population Size **2**

3 Calculation of Generation Time **2**

4 ODE Description of Model **4**

5 Fitness Measurements **5**

6 Comparison To Moran Model **6**

7 $\beta_{res} = 70$ Measurements **6**

1 Steady-States Are Independent of Initial Conditions

This section serves to verify that our choice of initial condition ($V_0 = 2B_0$) does not impact the steady-state phage population V_{ss} reached in the stochastic simulations. Fig. S1 shows that V_{ss} remains constant across a wide range of V_0 values, thereby confirming the choice of V_0 is not important.

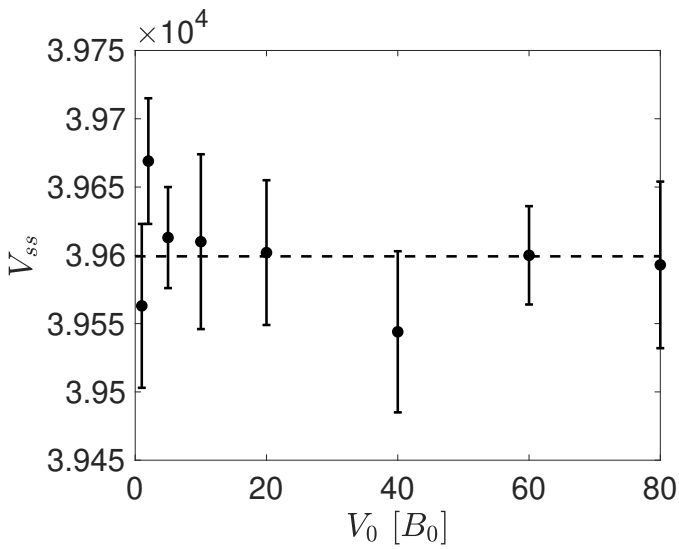

Figure S1. The steady-state phage population V_{ss} reached does not depend on the initial number of phage V_0 in the simulations. In all, $\alpha = 3 \times 10^{-6}$, $\beta = 100$, $\tau = 15$, $\delta = 0.1$ and $B_0 = 1000$.

2 Effective Population Size

Here we show an example of the average decay in heterozygosity $H = 2f(1-f)$, as a function of time, with f and $(1-f)$ representing the frequencies of two neutral labels in the population. We find (Fig. S2) that the heterozygosity decays exponentially at long times, consistent with previous work [1]: $H \propto e^{-2t/N_e}$. The decay rate, in units of generations (see Methods), is expressed in terms of an effective population size $2/N_e$ (Moran model [1]).

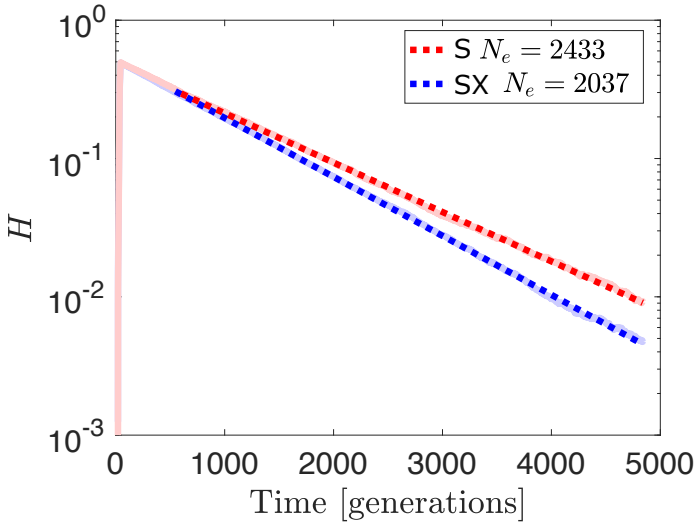

Figure S2. Linear fit to log transformed heterozygosity data, with slope $\Lambda \equiv 2/N_e$ revealing that allowing superinfection (red) results in a larger effective population size compared to the case where superinfection is prevented (blue). Parameters used were $\alpha = 3 \times 10^{-6}$, $\beta = 100$, $\tau = 15$, $\delta = 0.1$ and $B_0 = 1000$.

3 Calculation of Generation Time

In the main text we show that the generation time T can be written as

$$T = \tau + \frac{1}{\delta + \alpha I_{ss}}. \tag{1}$$

This yields $T = 24.80$ for the parameters used in the main text ($\alpha = 3 \times 10^{-6}$, $\tau = 15$, $\delta = 0.1$ and $I_{ss} = 681$).

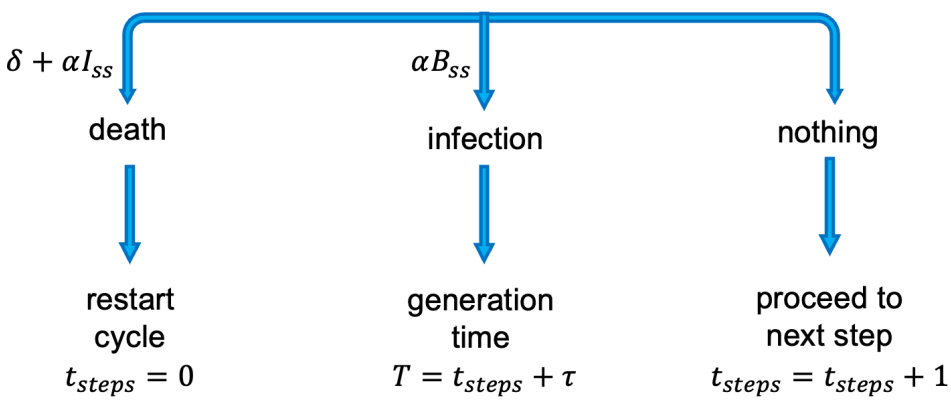

Figure S3. Schematic diagram illustrating the processes used to verify the generation time T in superinfection-excluding populations.

We here verify the results of this expression using stochastic simulations. We simulate a single phage, which in each time-step Δt has a probability of successfully adsorbing to an uninfected host ($\alpha B_{ss}\Delta t$), and a probability of *dying* ($(\delta + \alpha I_{ss})\Delta t$). In the event that the phage successfully adsorbs to a host before it dies, the number of steps t_{steps} taken for this to occur is noted, and the time $T = \tau + t_{steps}$ is recorded (representing the time between the 'birth' of the original phage and the 'birth' of it's offspring, as per the definition of generation time in the main text). A schematic representation of this process is shown in Fig. S3. This process was repeated 10 million times, with the the time T being recorded in all of the instances where the phage successfully reproduced. This yields an average generation time of $\overline{T} = 24.78(3)$ in agreement with the analytical calculation.

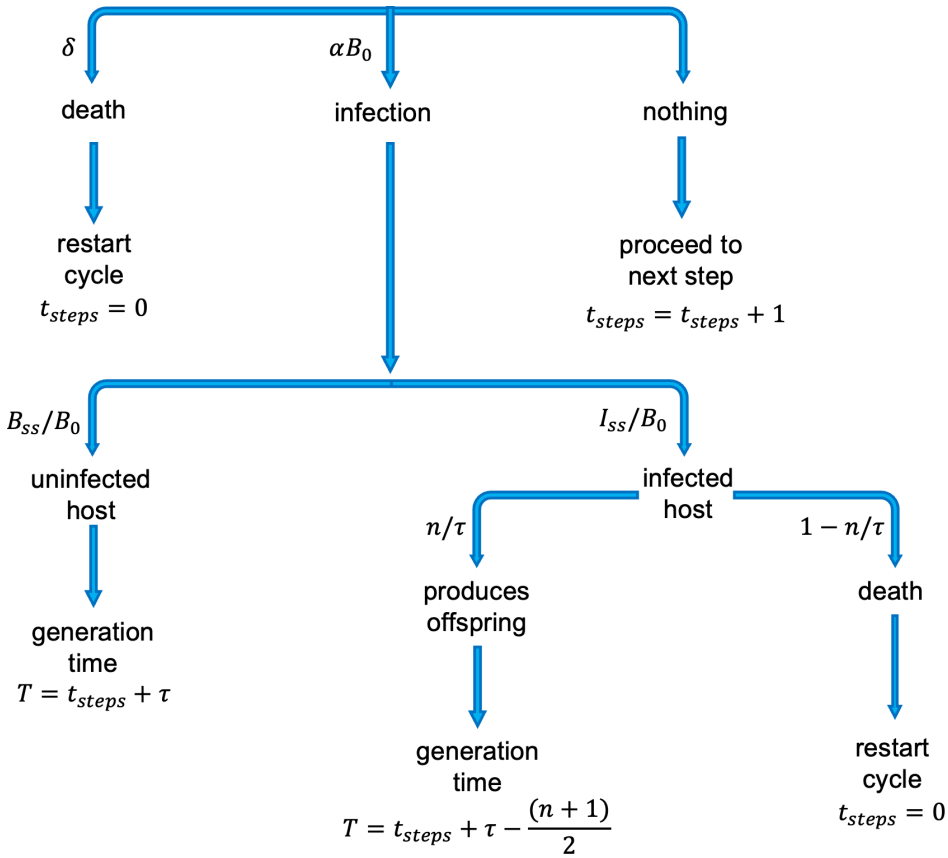

Figure S4. Schematic diagram illustrating the processes used to measure the generation time T in superinfecting populations.

Throughout the main text we use the above generation time for both superinfection-excluding and superinfecting populations. However, the superinfection scenario differs from that laid out above in that adsorption to infected cells does not result in death, and relatedly, the time between successful host infection and offspring production may be less than τ. To evaluate the error we introduce with our approximation of generation time, we modify the simple stochastic simulations above to take into account these differences. In this scenario, in a single time-step the phage has a probability $\delta\Delta t$ of dying, and a probability $\alpha B_0 \Delta t$ of infecting a host (either infected or uninfected). In the case where infection occurs, the phage has a probability B_{ss}/B_0 of infecting an uninfected host, which as before, results in a generation time $T = \tau + t_{steps}$. In the remainder of infection cases, phage will infect already infected hosts. Because of the nature of the process of within-host replication, secondary infections that occur too late after the initial infection generate almost no offspring of the superinfecting phage. We account for this observation by assuming that only secondary infections occurring within the first n steps post initial infection will successfully produce offspring. Given that we are considering populations at steady state, we assume that infected cells are equally likely to be found any number of steps post-infection ($< \tau$), and so infection a cell in the first n steps post initial infection simply occurs a fraction n/τ of the times that secondary infection occurs. In this case, the generation time is given by $T = t_{steps} + \tau - \frac{\sum_1^n k}{n}$, where the final two terms represent the average number of steps between secondary infection and lysis. This final

term can be simplified by noting that $\frac{\sum_1^n k}{n} = \frac{n(n+1)}{2n} = \frac{n+1}{2}$. A schematic representation of this process is shown in Fig. S4.

Using a value of $n = 3$, this process was again repeated 10 million times, yielding an average generation time of $\overline{T} = 24.11(3)$. It can be seen that the difference in generation time is marginal. It is however worth noting that were we to fully account for the shorter generation time in superinfecting populations, it would result in an even larger effective population size, further emphasising our main findings.

4 ODE Description of Model

The average behaviour of the model used in the main text can be described by a set of ordinary differential equations (ODEs):

$$\frac{dV}{dt} = -\alpha V(B+I) - \delta V + \beta\alpha V_{t-\tau}B_{t-\tau}, \tag{2a}$$

$$\frac{dB}{dt} = -\alpha VB + \alpha V_{t-\tau}B_{t-\tau}, \tag{2b}$$

$$\frac{dI}{dt} = \alpha VB - \alpha V_{t-\tau}B_{t-\tau}, \tag{2c}$$

where all of the symbols are defined the same as in the main text (V, B and I indicate the concentrations of phage, uninfected bacteria and infected bacteria as a function of time respectively; α, β, τ and δ indicate the phage adsorption rate, burst size, lysis time and decay rate respectively). The subscript is used to indicate that those terms are calculated at time $t - \tau$. The positive term in Eq. 2b accounts for the instantaneous replacement of lysed cells in our turbidostat environment.

By numerically solving this ODE system, we can verify that for the parameters used in this work, a steady state solution is reached where $V = V_{ss}$, $B = B_{ss}$ and $I = I_{ss}$, in agreement with the average behaviour of the stochastic model used throughout the main text (Fig. S5 and Fig. S6).

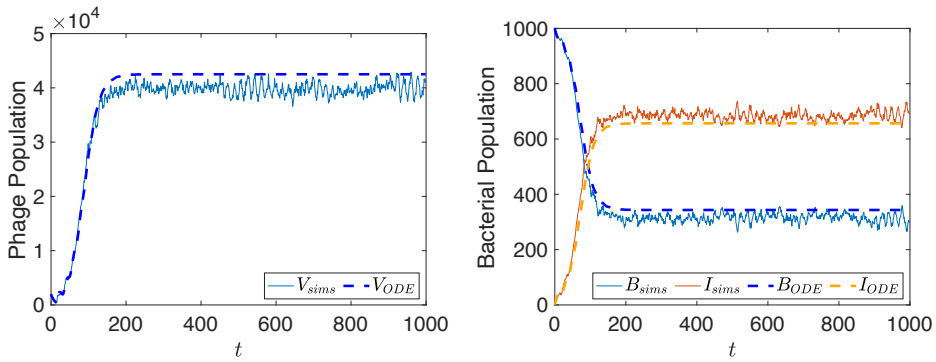

Figure S5. The average behaviour of the model in the main text is mostly captured by the ODE description set out in Eqs. 2. Slight discrepancies probably arise from the discreteness of the infection, decay and lysis steps in the simulations. Parameters used are $\alpha = 3 \times 10^{-6}$, $\beta = 100$, $\tau = 15$, $\delta = 0.1$ and $B_0 = 1000$.

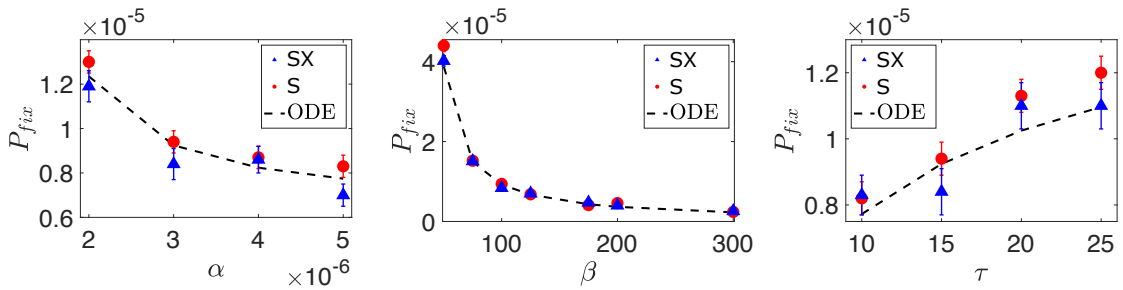

Figure S6. Probability of mutant fixation P_{fix} in the superinfection (S) and superinfection-exclusion (SX) scenarios as a function of adsorption rate α, burst size β and lysis time τ. This is the same as the data displayed in Fig. 3 of the main text, prior to rescaling by the initial frequency $f_0^* = 1/(V_{ss} + \beta I_{ss})$. Error bars are plotted, although in some instances may be too small to see. This data is compared with the solution of the system of ODEs, where the black dashed line represents the frequency f_0^* calculated from the steady-state values.

5 Fitness Measurements

In Fig. S7 we present the fitness measurements made using our stochastic model, as the phage infection parameters (adsorption rate α, burst size β and lysis time τ) are varied. As described in the main text, fitness is measured both in terms of its effect on the growth rate in isolation (s_{growth}), and in terms of its effect in a competitive setting, by the relative change in frequency of two variants in a population (s_{SX} and s_S).

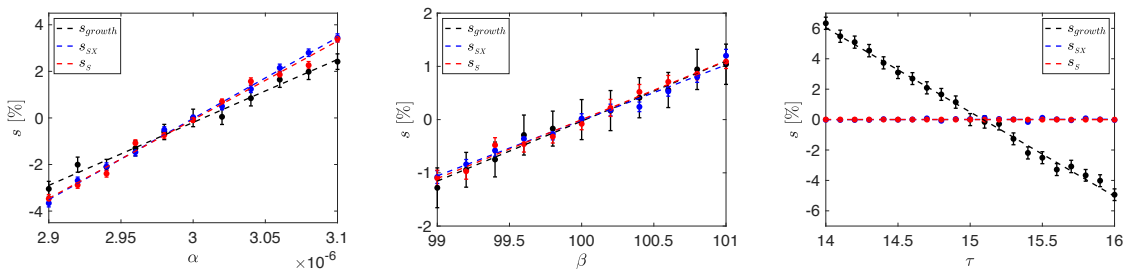

Figure S7. The selective advantage s relative to a resident phage that results from a change to adsorption rate α, burst size β and lysis time τ. This is measured both in terms of the effect on the isolated growth rate of the mutant (s_{growth}, Eq. 7), and in terms of the change in frequency in a population initiated with 50% mutant and 50% resident (s_{SX} and s_S, Eq. 9). Resident parameters used were $\alpha = 3 \times 10^{-6}$, $\beta = 100$ and $\tau = 15$. As before $\delta = 0.1$ and $B_0 = 1000$.

In Fig. S8 we show using the ODE model, which describes the average behaviour of the system, that once the system has reached steady-state, altering lysis time has no impact on the relative frequency of two variants within the population (i.e. both variants appear neutral relative to one another). This supports the observation in the stochastic model that $s_{comp}(\tau) \approx 0$.

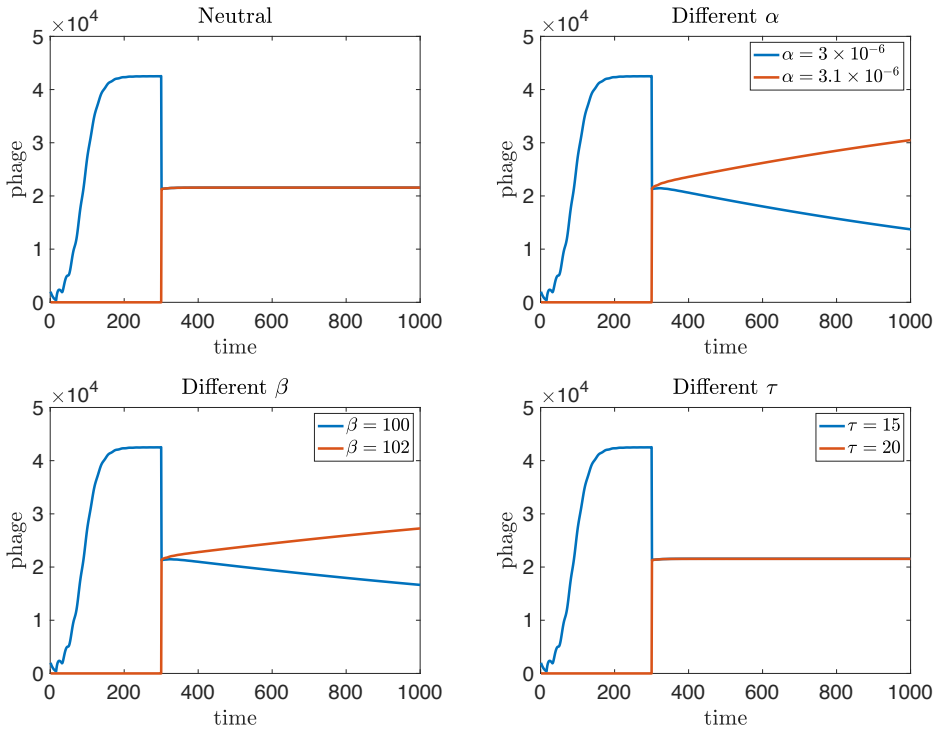

Figure S8. The relative change in frequency of two populations in the ODE model (indicating the average behaviour in the stochastic model). It can be seen that once at steady-state, changing lysis time τ has no effect. Parameters used were $\alpha = 3 \times 10^{-6}$, $\beta = 100$ and $\tau = 15$ unless otherwise stated. As throughout, $\delta = 0.1$ and $B_0 = 1000$.

6 Comparison To Moran Model

If we introduce a free scaling parameter ϕ, such that $s = \phi s_{comp}$, and optimally fit Eq. 10 to the data, we can use the resulting value for ϕ as a quantitative measure of the quality of agreement between simulations and theory. It should be noted that while we have described the scaling in terms of s, it is mathematically identical to scaling N_e. Through this optimal fitting we find that $\phi_{SX\alpha} = 1.050$, $\phi_{SX\beta} = 1.028$, $\phi_{S\alpha} = 0.992$ and $\phi_{S\beta} = 0.986$, with subscripts indicating scenario and parameter combinations. This indicates that both scenarios agree with the Moran model to within 5%.

7 $\beta_{res} = 70$ Measurements

Here we repeat a subset of the measurements carried out in the main text for different resident phage parameters, in this instance $\beta_{res} = 70$, with all other parameters remaining the same as in the main text. First, the effective population size is measured in both superinfecting and superinfection-excluding populations (Fig. S9), demonstrating that N_e is larger in superinfecting populations.

We then move on to characterise the fitness of non-neutral mutants, in this instance only varying burst size β (Fig. S10). Again, we find a positive linear relationship between burst size and fitness, both in terms of the effect on growth rate in isolation and in a competitive setting. Interestingly here we find that alterations to burst size make slightly less difference in a competitive setting, as compared to the effect on growth rate. This could potentially be because, at lower burst sizes, any small change in β has a large impact on the growth rate, but has a smaller impact in a population already at steady state.

Finally, we put both aspects together and measure the probability of fixation of non-neutral mutants in both superinfecting and superinfection-excluding populations (Fig. S11). As in the main text, we find fairly good, although slightly worse, agreement between our simulation results and the prediction from a Moran model with our independently measured parameters (Fig. S9 and Fig. S10). In terms of the additional fitting parameter introduced in the previous section, we find here that $\phi_S = 0.83$ and $\phi_{SX} = 0.90$. It's possible that this discrepancy is caused by imprecision in the measurements of fitness as a function of burst size. Indeed, over the whole range of β we would not expect a perfect linear

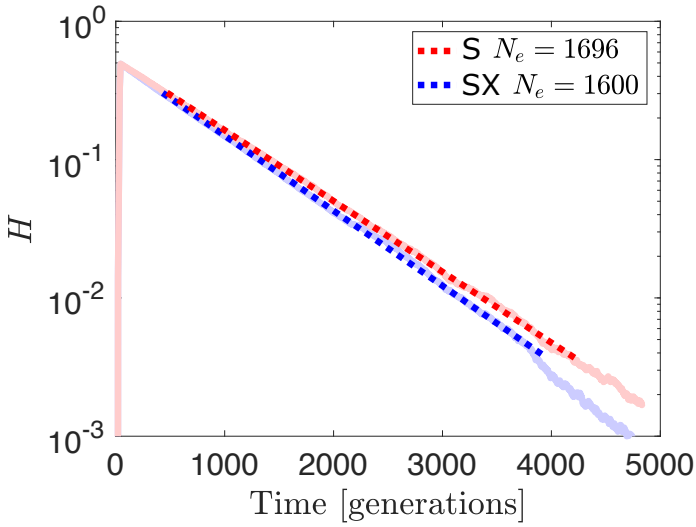

Figure S9. Linear fit to log transformed heterozygosity data, with slope $\Lambda \equiv 2/N_e$ revealing that allowing superinfection (red) results in a larger effective population size compared to the case where superinfection is prevented (blue). Parameters used were $\alpha = 3 \times 10^{-6}$, $\beta = 70$, $\tau = 15$, $\delta = 0.1$ and $B_0 = 1000$.

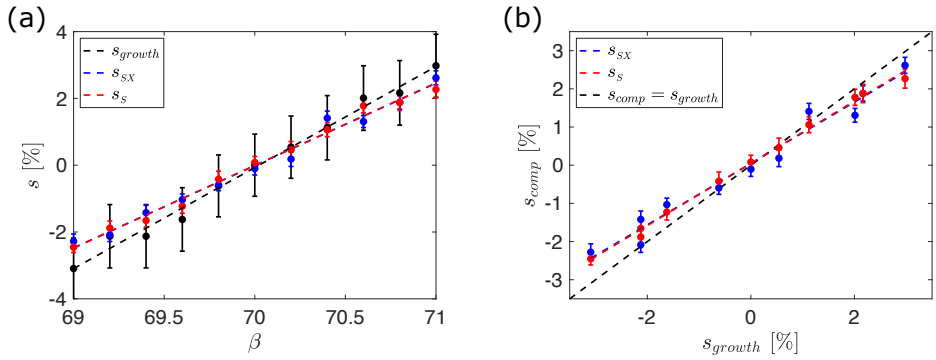

Figure S10. (a): The selective advantage s relative to a resident phage that results from a change to burst size β. This is measured both in terms of the effect on the isolated growth rate of the mutant (s_{growth}, Eq. 7), and in terms of the change in frequency in a population initiated with 50% mutant and 50% resident (s_{SX} and s_S, Eq. 9). (b): The fitness in a competitive setting s_{comp} is then shown as a function of the fitness in an isolated setting s_{growth}. Resident parameters used were $\alpha = 3 \times 10^{-6}$, $\beta = 70$ and $\tau = 15$. As before $\delta = 0.1$ and $B_0 = 1000$.

relationship between burst size and fitness, with the benefits of increased burst size being larger for small β, and so at these lower values of β we find that the linear fit is less of a good approximation.

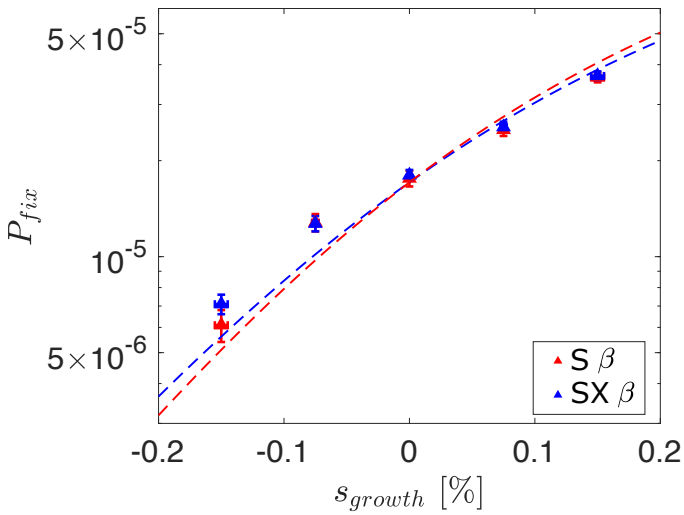

Figure S11. Probability of mutant fixation P_{fix} as a function of selective growth advantage s_{growth}. Points indicate simulation results, while lines indicate theoretically predicted values in a Moran model with equivalent parameters (Eq. 10).

References

[1] P. A.P. Moran. Random processes in genetics. *Mathematical Proceedings of the Cambridge Philosophical Society*, 54(1):60–71, 1958.